


Article

Enhancing Wireless Power Transfer Efficiency Through Innovative Metamaterial Configurations for Electric Vehicles

Wandee Onreabroy¹, Supatsara Piemsomboon², Suneerat Traikunwaranon², Naksit Wilaiprajuabsang² and Amornrat Kaewpradap^{2,*} 

¹ Department of Physics, Faculty of Science, King Mongkut's University of Technology Thonburi, 126 Pracha Uthit Road, Bang Mod, Thung Khru, Bangkok 10140, Thailand

² Combustion and Energy Research Laboratory (CERL), Department of Mechanical Engineering, Faculty of Engineering, King Mongkut's University of Technology Thonburi, 126 Pracha Uthit Road, Bang Mod, Thung Khru, Bangkok 10140, Thailand

* Correspondence: amornrat.kae@kmutt.ac.th

Abstract: This study investigates the enhancement of power transfer efficiency (PTE) in wireless power transfer (WPT) systems for electric vehicles (EVs) through simulations and experimental evaluations using metamaterial (MTM) configurations. The MTM model, validated against existing research, was designed for operation at 85 kHz. The influence of MTM on the magnetic field alignment and flux density at the receiver coil significantly improved PTE compared to systems without an MTM configuration. We tested various arrangements of three, six, and nine MTM cells positioned at left, right, top, bottom, and combined locations across coil distances of 0–5.0 cm. The results showed that a nine-cell MTM arrangement yielded greater PTE than a three-cell arrangement because of improved electromagnetic flux distribution. However, the T-shaped arrangement of six MTM cells achieved the maximum PTE at a 2.0 cm coil distance. This performance exceeded that of the configuration with 3×3 MTM cells, indicating that the T-shaped design optimizes electromagnetic flux distribution. The six-cell T-shaped arrangement boosted the PTE by 7.7% compared to the nine-cell version, demonstrating its potential as an innovative and efficient WPT system for future EV applications.

Keywords: metamaterial; wireless power transfer efficiency; wireless charger; electromagnetic flux; electric vehicle



Academic Editor: Michael Fowler

Received: 25 December 2024

Revised: 13 January 2025

Accepted: 16 January 2025

Published: 19 January 2025

Citation: Onreabroy, W.; Piemsomboon, S.; Traikunwaranon, S.; Wilaiprajuabsang, N.; Kaewpradap, A. Enhancing Wireless Power Transfer Efficiency Through Innovative Metamaterial Configurations for Electric Vehicles. *World Electr. Veh. J.* **2025**, *16*, 48. <https://doi.org/10.3390/wevj16010048>

Copyright: © 2025 by the authors. Published by MDPI on behalf of the World Electric Vehicle Association. Licensee MDPI, Basel, Switzerland. This article is an open access article distributed under the terms and conditions of the Creative Commons Attribution (CC BY) license (<https://creativecommons.org/licenses/by/4.0/>).

1. Introduction

Among the various electric vehicles (EVs) available, battery EVs (BEVs) boast the highest energy efficiency, converting up to 80% of the energy stored in the battery into kinetic energy. The electric motor is highly efficient, and BEVs also recover braking energy that would otherwise be lost as heat in internal combustion engine vehicles (ICEVs), converting it into usable kinetic energy [1–3]. BEVs produce no emissions during operation, and their environmental impact is further reduced when the electricity used to charge them comes from renewable sources.

However, BEVs face challenges such as limited range, long charging times, and reliance on batteries that contain rare minerals [1,3]. The studies by Del Pero et al. [4] and Peng et al. [5] highlighted that BEVs can significantly contribute to reducing carbon emissions in the transportation sector. Another study examined the potential of EVs (BEVs and plug-in hybrid EVs (PHEVs)) to reduce CO₂ emissions, revealing that their impact varies

depending on the technology used. BEVs were found to be more effective at minimizing CO₂ emissions compared to PHEVs [6].

BEVs, which have large battery banks with a long charging duration and energy consumption capacity, and PHEVs, which have a smaller battery capacity, are charged on the grid [7]. EVs are primarily powered by an electric motor, which draws energy from a battery that can be charged using conductive charging or wireless charging (using electromagnetic induction). Conductive charging, which requires a physical connection between the battery and a power source, is very efficient for delivering high power. However, it has several drawbacks, including the need to plug and unplug the charger, cumbersome cables, the risk of improper connections, cable damage, interruption of charging due to tripping, and wear on electrical connectors due to high currents [8]. To overcome these challenges, researchers developed wireless charging, which enables power transfer through methods such as electromagnetic induction, magnetic resonance, electric field coupling, and radio wave reception [9]. The wireless power transfer (WPT) system delivers electricity to portable devices using an electromagnetic induction field between the transmitter and receiver coils. However, WPT has a lower transfer efficiency compared to conductive charging [10,11].

Wireless charging is currently limited by the magnetic field energy transfer distance between the transmitter and receiver coils. Therefore, many studies and patents have addressed the development of rectifier circuits, high-frequency magnetic field wire loops, and receiver wire loops to achieve a high-power-induced electromagnetic field [12,13]. Induction coupling and the implementation of two coils were investigated for WPT to reduce energy use [14,15]. Another study investigated coils of different parameter geometries, such as circular, rectangular, and hexagonal, in relation to WPT for EV charging systems [16]. Recent works showed the effects of distance on WPT, and nearfield communication was applied using a current-controlled loop with a loaded capacitance [17,18]. In addition, researchers studied the induction of efficient far-field WPT via field-shaping techniques and reducing coil misalignment to enhance power transfer efficiency (PTE) [19,20]. Recently, the application of WPT to electric vehicle charging systems was investigated, specifically the limitations of the distance between the transmitter and receiver coils.

To enhance PTE in EVs, engineers have designed and utilized metamaterials (MTMs) to improve the electromagnetic path [21]. Previous research demonstrated that the use of MTMs significantly optimized WPT performance [22]. A simulation of wireless power systems was conducted using inhomogeneous MTMs to analyze the impact of electromagnetic parameters on PTE [23]. Recently, magnetic megahertz-range MTMs were designed, and their effects on power transmission systems were examined [24–26]. In addition to simulations, experimental investigations were carried out on 1D, 2D, and 3D MTMs applied at 6.78 MHz in WPT systems [27].

As mentioned above, MTMs are crucial for improving the PTE of EV charging systems. However, explorations of the impact of the MTM design and arrangement on electromagnetic paths, electromagnetic flux, WPT, and PTE are lacking, making it an important area of investigation for advancing EV charging applications. Therefore, this study focuses on how the design and arrangement of MTMs affect the electromagnetic paths, electromagnetic flux, and PTE in a WPT model. Validation is conducted against a reference MTM, and an experimental study on the design and arrangement of MTMs is conducted to enhance the PTE of the WPT system.

2. Methodology

Our investigation of the MTM's impact on WPT involved both simulations and experiments. First, we conducted a simulation study on an MTM model and then validated it against a referenced model [16]. Next, we performed an experimental study to examine the

effect of the MTM arrangement on the WPT system. To further analyze the effect of the MTM on WPT, we arranged a series of suitable MTM configurations and experimentally tested them to evaluate the WPT efficiency and PTE in the wireless power system. The MTM was specifically designed to enhance the effective permeability μ_{eff} at 85 kHz for improved WPT. The performance of the WPT model with the optimized MTM was thoroughly investigated and compared to a WPT model without an MTM. The methodology of this study is outlined as follows.

2.1. MTM Model

The efficiency of an MTM is primarily influenced by two factors: natural resonance frequency and resonance intensity. To achieve resonance, engineers commonly employ split-ring resonators (SRRs) because of their specialized structure, which supports resonant interactions with magnetic fields. In this study, a double-square SRR is used for the MTM design. A split-ring resonator consists of concentric metal rings with gaps that allow them to resonate at specific frequencies when exposed to an electromagnetic field. When the magnetic field oscillates at the resonant frequency of the SRR, the resonator becomes highly effective at coupling with the field, enhancing the magnetic response and improving the system's efficiency. The double-square SRR design further fine-tunes the resonance behavior by adding an extra layer of complexity, which allows for better control over the interaction of the magnetic field with the MTM [28].

2.2. Effective Permeability

MTMs are artificial materials engineered to achieve electromagnetic properties that are not found in nature, often by manipulating their effective permeability (μ_{eff}), as presented in Equation (1). In certain frequency ranges, MTM can exhibit a negative effective permeability, typically achieved using structures like split-ring resonators (SRRs). These properties strongly influence the impedance (Z) and refractive index (n), leading to unique wave propagation behaviors. The wave impedance of a medium is the ratio of the electric field (E) to the magnetic field (H) in a traveling electromagnetic wave, as shown in Equation (2). The refraction effective permeability can be engineered using structures like split-ring resonators (SRRs) to achieve values that are not possible in natural materials. The refractive index is determined by the relative permeability (μ_r) and relative permittivity (ϵ_r) of the material, as illustrated in Equation (3).

$$\mu_{\text{eff}} = nz \quad (1)$$

$$z = \frac{E}{H} \quad (2)$$

$$n = \sqrt{\mu_r \epsilon_r} \quad (3)$$

2.3. WPT Efficiency

The PTE η_{PTE} can be defined using the coupling coefficient K , the quality factor of the transmitter (T_x) coil Q_1 , and the quality factor of the receiver (R_x) coil Q_2 , as shown in Equation (4); the quality factor of each coil can be calculated using Equation (5), obtained from the frequency of the magnetic field f , the coil inductance L , and the coil resistance R . Following the PTE equation, the quality factor in WPT systems is a measure of how effectively a resonator stores energy relative to how much energy it dissipates per cycle. When the quality factor is higher, the coupling between the transmitter and receiver at resonance could be enhanced, enabling longer power transfer distances. For magnetic

resonance coupling, a high-quality factor could support efficient energy transfer, even when coils are spaced further apart.

$$\eta_{PTE} = \frac{1}{1 + \left(\frac{2}{k^2 Q_1 Q_2}\right) + \left(\frac{2\sqrt{k^2 Q_1 Q_2 + 1}}{k^2 Q_1 Q_2}\right)} \quad (4)$$

$$Q = \frac{2\pi f \cdot L}{R} \quad (5)$$

3. Simulation and Experimental Studies

3.1. Simulation Study

Figure 1 illustrates the characteristics of the T_x and R_x coils, including their specific coil distances and diameters. Power is transferred between two coils, typically a transmitter and a receiver, via a magnetic field. This magnetic field is generated by the alternating current (AC) flowing through the transmitting coil. The magnetic flux generated by this current induces a voltage in the receiver coil, allowing for WPT. WPT also relates to the total electromagnetic field, which includes electric and magnetic fields passing through a surface.

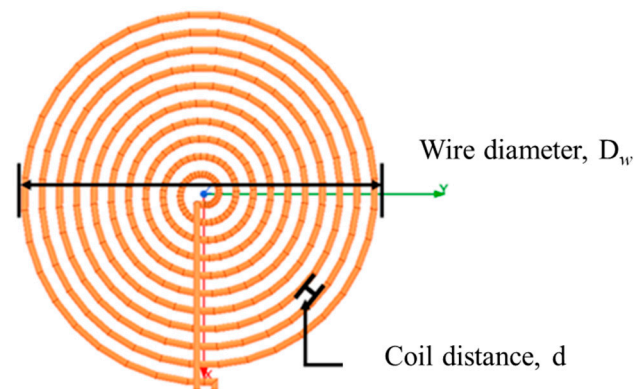


Figure 1. Characteristics of T_x and R_x coils.

Figure 2 presents the WPT model, which consists of T_x and R_x coils, analyzed using Ansys Electronics Desktop Student. They have a wire diameter of 150 μm , and both coils have a diameter of 1.3 mm and a coil distance of 0 mm. The coupling coefficient K between the transmitter and receiver coils was set to 0.76. The specifications of the T_x and R_x models are shown in Table 1.

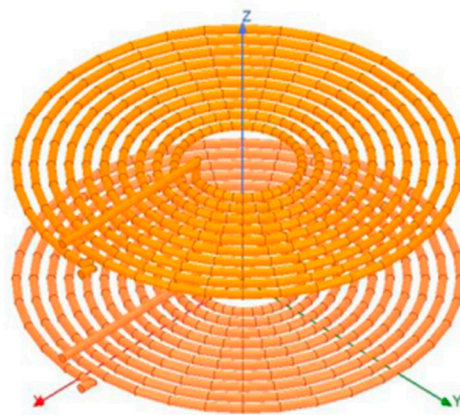


Figure 2. Model of transmitter and receiver coils.

Table 1. Specifications of T_x and R_x coils.

Specifications	Value
T_x coil diameter D_T (mm)	1.3
R_x coil diameter D_R (mm)	1.3
T_x coil inductance L_T (μH)	4.6015
R_x coil inductance L_R (μH)	2.7377
Coupling coefficient K	0.76

Following [23], the simulation results, including the effective permeability μ_{eff} of the MTM model, were obtained and compared. Figure 3 illustrates the parameters of the SRR, including the conductor width w , the gap between conductor rings s , the split gap g , the length of the conductor ring l , the number of rings N , the magnetic permeability effectiveness μ_0 , the substrate thickness h , and the thickness of the conductor t . Table 2 shows the specification of the MTM designed for the WPT system. To further enhance the PTE, the high-conductivity material and resonator geometry were considered to obtain the MTM structure for this study. The MTM in this study was designed using a double-square SRR and implemented with a copper material plate and printed circuit board (PCB). Metamaterials consist of sub-wavelength structures like SRRs and wire arrays, which introduce losses due to ohmic resistance caused by the finite conductivity of materials such as copper. The impact of the MTM results in high intrinsic losses, leading to significant power dissipation and reduced efficiency in power transfer systems. As the numerical model, the designed MTM was applied between the transmitter and receiver coils to enhance the magnetic field and PTE. The MTM integrated into the WPT system is shown in Figure 4.

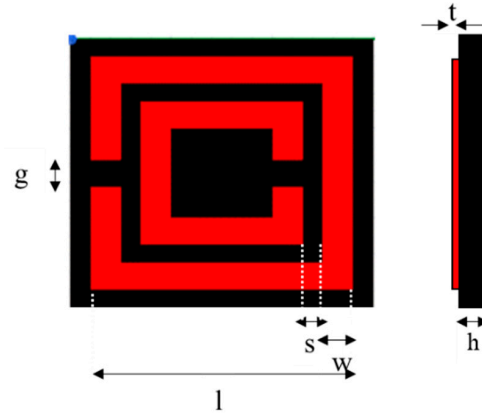
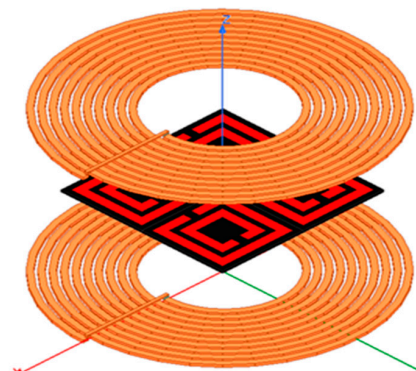
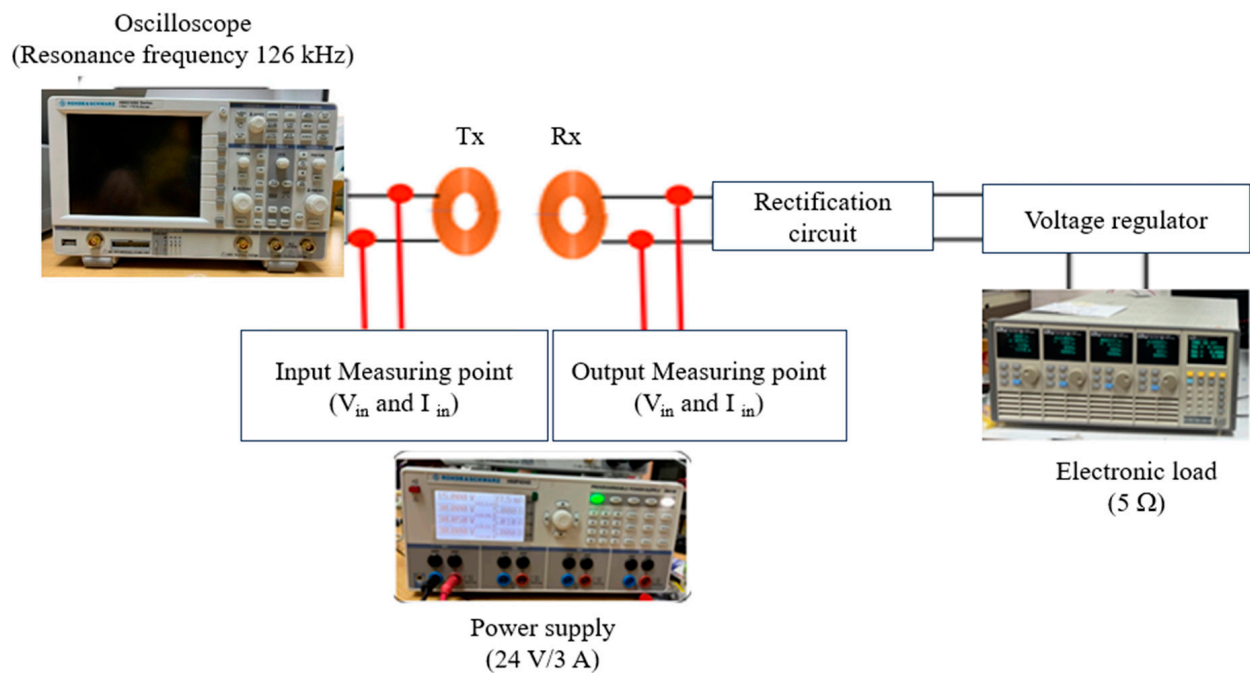
**Figure 3.** Parameters of SRR for MTM model.**Figure 4.** WPT model with MTM.

Table 2. Specification of MTM designed for WPT system.

MTM Specification	Parameter	Unit	Value
Length of conductor ring	l	mm	26.0
Split gap	g	mm	3.0
Gap between conductor rings	s	mm	2.0
Substrate thickness	h	mm	0.8
Conductor width	w	mm	3.0
Thickness of the conductor	t	mm	0.035
Number of rings	N	-	2
PCB material	-	-	Copper
Substrate material	-	-	FR-4

3.2. Experimental Apparatus

The experimental setup for the WPT system is depicted in Figure 5. This setup includes a wireless charging module, which consists of the T_x and R_x coils and the designed MTM. The MTM model was validated against referenced studies and specifically designed to operate at 85 kHz. As shown in Figure 6, the experimental arrangement positions the T_x and R_x coils and the MTM in specific locations. The MTM is placed between the transmitter and receiver coils to optimize power transfer.

**Figure 5.** Experimental setup of WPT system.

Power measurements at the input (transmitter) and output (receiver) were recorded using an oscilloscope, which captured the power levels of both the transmitter and receiver coils during the experiment. This experimental arrangement was designed to evaluate the performance of the wireless power system with and without the MTM. By analyzing the PTE in this setup, we could assess the effect of the MTM on the performance of the system, with the oscilloscope serving as the primary tool for measuring and comparing the transmitted and received power levels. We studied MTM configurations consisting of three, six, and nine MTM cells arranged at various positions (left, right, top, and bottom). These configurations are abbreviated as MT-3L, MT-3R, MT-3T, MT-3B, MT-3VM, MT-3HM, MT-6LT, MT-6T, MT-6ML, and MT-9F, as defined in Figure 7.

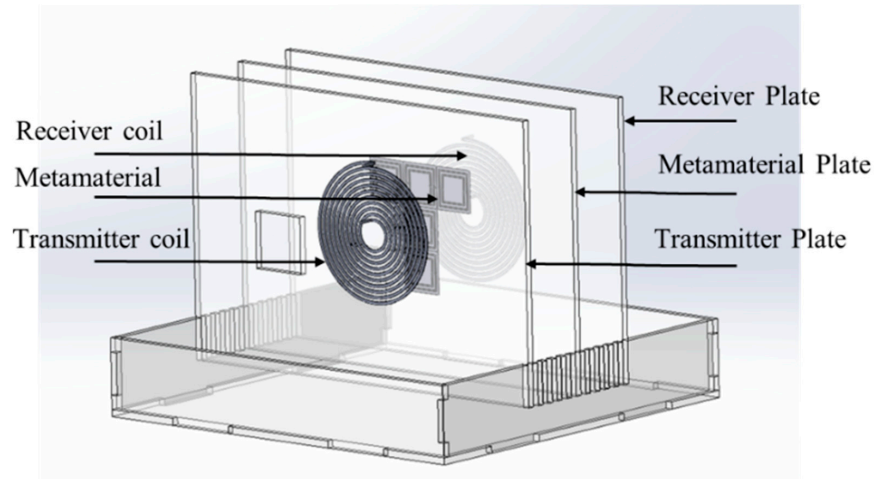


Figure 6. Locations of T_x coil, R_x coil, and MTM in experimental setup.

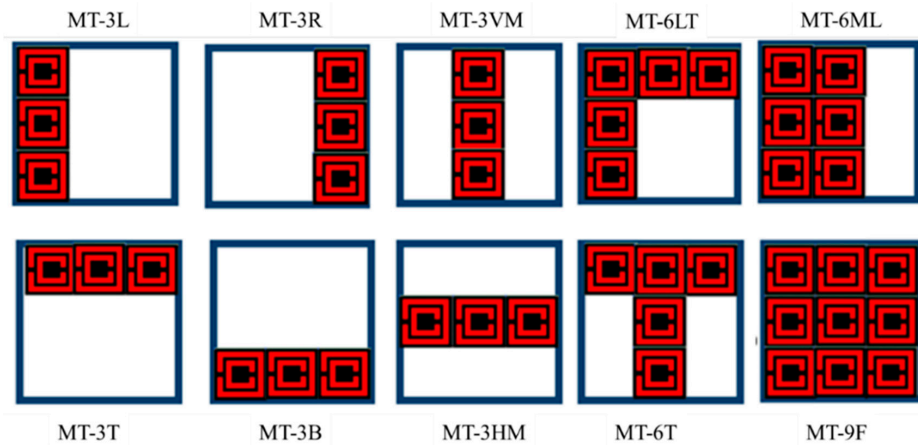


Figure 7. Arrangements of three, six, and nine MTM cells.

4. Results and Discussion

4.1. Validation of MTM Model

Following the model of transmitter and receiver coils, the PTE was investigated at coil distance 0 and 2 mm as shown in Table 3. As the coil distance increased, the PTE decreased due to lower magnetic flux density. In order to enhance the magnetic flux density, MTM was set between transmitter and receiver coils.

Table 3. PTE between transmitter and receiver coils model at coil distances of 0 and 2 mm.

Specifications	Case 1	Case 2
T_x coil diameter D_T (mm)	1.3	1.3
R_x coil diameter D_R (mm)	1.3	1.3
Coil distance d (mm)	0	2
PTE η_{PTE} (%)	97.86	93.58

Based on the study by Smith et al. [23], an MTM model was designed to investigate its effective permeability. Figure 8 presents a comparison of the numerical effective permeability between the present study and the referenced study at a frequency of 20 MHz. The results show that the effective permeability of the MTM model in this study aligns closely with that from the referenced study, validating the accuracy of the numerical model. This validation confirms that the MTM model used in this study is reliable and can be effectively applied to explore the enhancement of PTE in WPT systems. The next step was

to investigate how this validated MTM model can improve the PTE by optimizing the interaction between the transmitter and receiver coils in the WPT system.

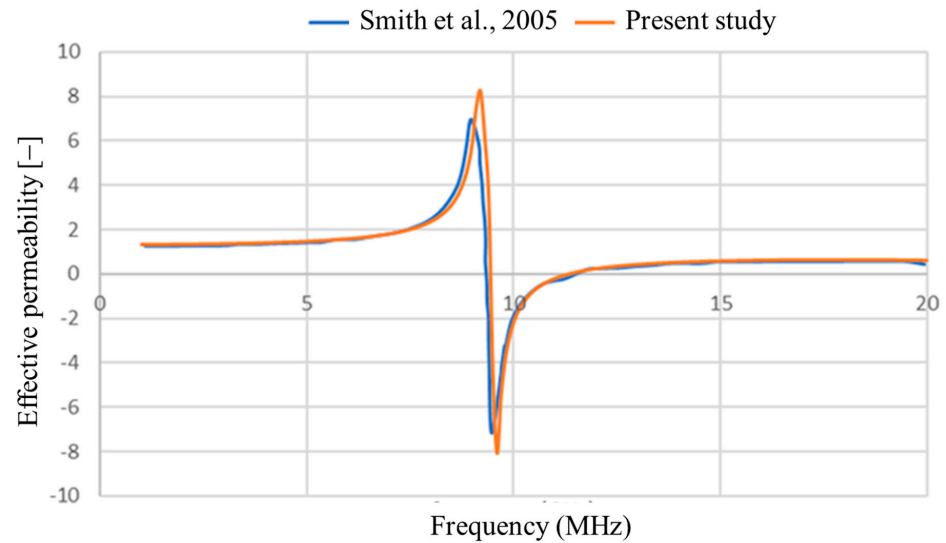


Figure 8. Comparison of effective permeability of MTM between present study and referenced study, data source from Ref. [23].

4.2. Enhancement of WPT Model with MTM

The MTM model was designed to be placed between the T_x and R_x coils in the WPT system. Table 3 shows the calculated PTEs at coil distances of 0 and 2.0 mm. The simulation results show that an initial PTE of $\sim 98\%$ was achieved when the coils were positioned 0 cm apart. When the coil distance increased to 2.0 mm, the resulting PTE was slightly lower compared to the closer coil distance, owing to less magnetic flux distribution.

To further enhance the PTE, the MTM was integrated into the WPT system. The simulation results demonstrated that the MTM played a crucial role in reducing electromagnetic flux leakage and directing the electromagnetic path more efficiently. Figures 9 and 10 compare the electromagnetic flux in the WPT system with and without the MTM. The results indicate that the MTM significantly reduces electromagnetic leakage, leading to a more concentrated magnetic flux. This improvement in magnetic flux distribution directly contributes to a higher PTE, highlighting the positive impact of the MTM on the overall WPT performance.

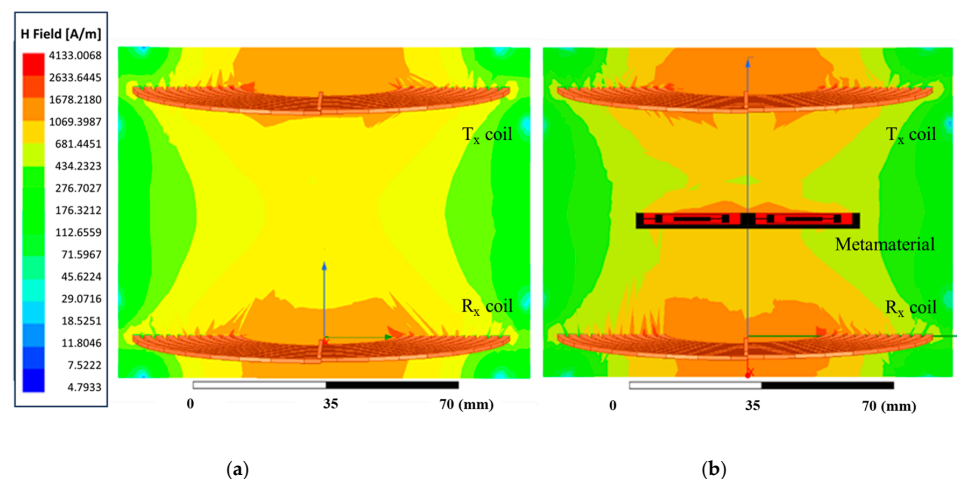


Figure 9. Electromagnetic fluxes on WPT: (a) without MTM and (b) with MTM.

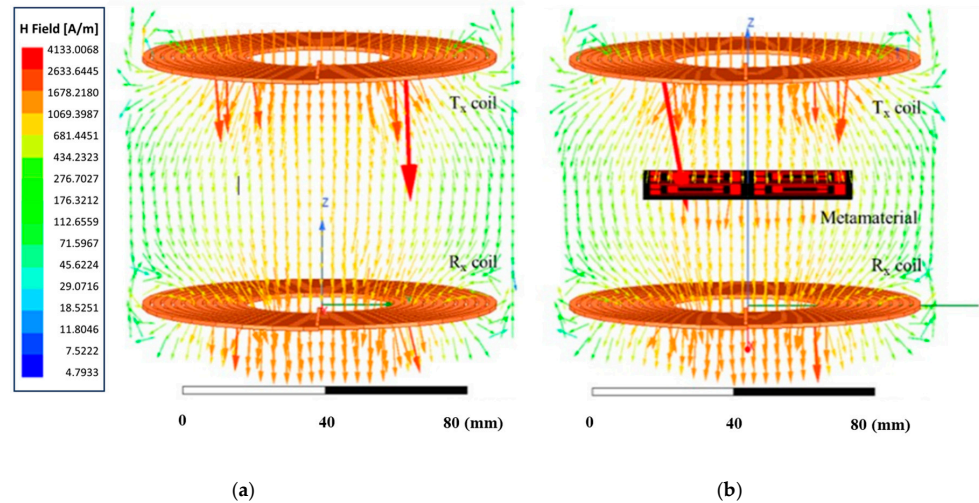


Figure 10. Vectors of electromagnetic field WPT: (a) without MTM and (b) with MTM.

4.3. Effects of MTM Cell Number

In the experimental study of the small WPT circuit, the negative effective permeability was observed at 126 kHz. Then, the WPT experiment using a power supply (24 V and 3 A) with circuit resistances of 1, 2, 3, 4, and 5 Ω at a coil distance of 0 cm was conducted and compared to the simulation results. Table 4 shows a comparison of the PTE between the experimental and simulation results. The experimental PTE (96.90%) at 5 Ω was the highest and closest to the simulation PTE (97.86%). Thus, the obtained results show that an experimental WPT setup with a circuit resistance of 5 Ω can be applied with an outcome comparable to the simulation results. The relationship between coil distance and PTE is presented in Figure 11. The experimental results indicate that the PTE varied with coil distances between 0 and 5.0 cm. More than 20% of the PTE was observed at a coil distance of 2.0 cm; thus, this distance was chosen as the reference for further experiments in this study. WPT experiments with these MTM arrangements were conducted at distances between the T_x and R_x coils ranging from 0 to 5.0 cm.

Table 4. Comparison of PTE between WPT model and WPT experiment with circuit resistances of 1, 2, 3, 4, and 5 Ω at a coil distance of 0 cm.

Load (Ω)	η_{PTE}
1	65.27%
2	76.14%
3	71.55%
4	84.19%
5	96.90%
Simulation	97.86%

In this study, three, six, and nine cells of MTM were analyzed to compare the PTE at a 2.0 cm coil distance to WPT without the MTM, as shown in Figure 12. The results showed that the WPT with MTM could enhance the PTE because the MTM rings resonated at the WPT frequency, enhancing inductive coupling and affecting the enlargement of magnetic field distribution for power transfer. The arrangement with nine MTM cells (MT-9F) achieved higher PTE compared to the arrangements with three MTM cells (MT-3L, MT-3R, MT-3T, MT-3B, MT-3VM, and MT-3HM), likely because of the increased number of cells and better distribution of electromagnetic flux. However, the highest PTE was observed with six MTM cells, indicating that the arrangement rather than the number of cells has a more significant impact on performance.

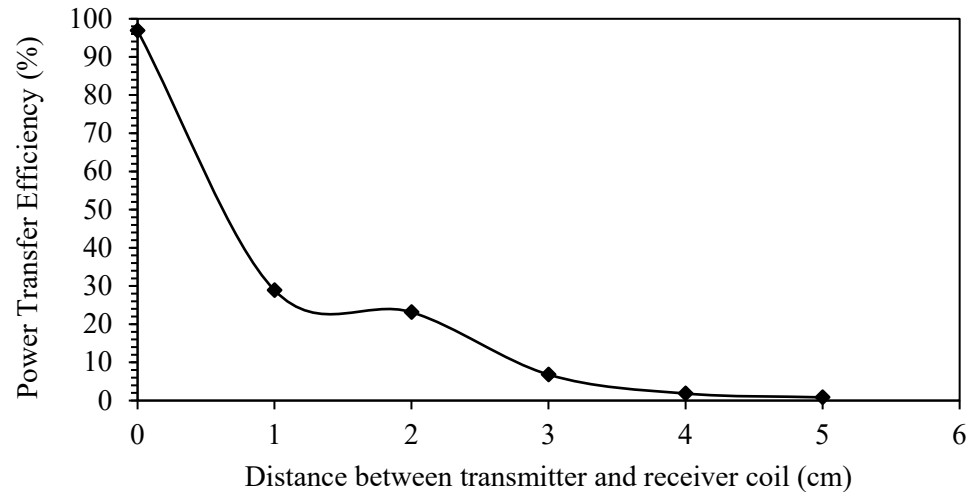


Figure 11. PTE vs. coil distance without MTM.

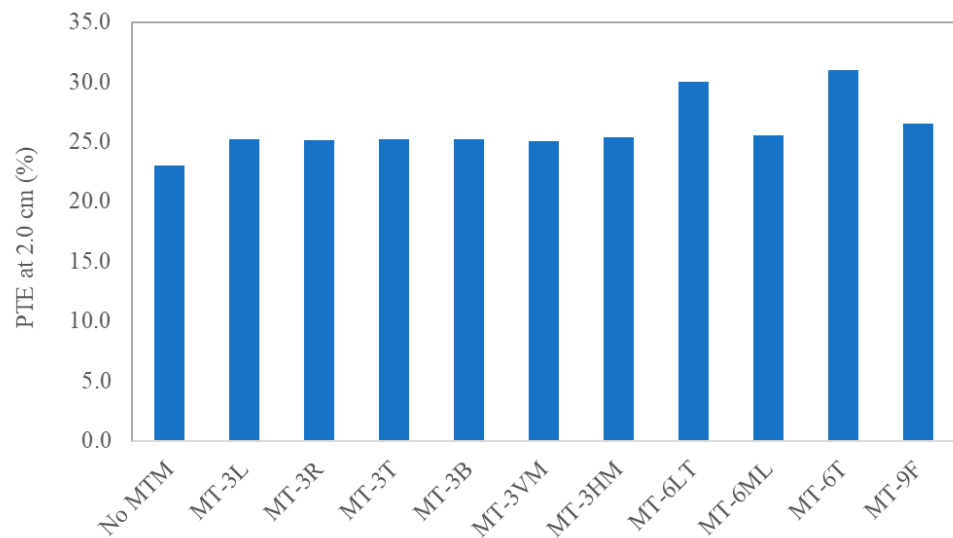


Figure 12. PTE at 2.0 cm coil distance for WPT with and without MTM arrangements.

4.4. Effects of MTM Cell Arrangement

The maximum PTE was observed with six MTM cells, leading us to focus on the cell arrangement. The PTEs of the six- and nine-cell configurations are plotted in Figure 13 as functions of coil distance. At a 2.0 cm coil distance, the MT-6T (T-shape with six cells) arrangement achieved the maximum PTE. Although the number of MTM cells plays a role in determining PTE, the distribution of electromagnetic flux is also heavily influenced by the specific arrangement of the MTM. The results show that the T-shaped arrangement of six MTM cells provided a higher PTE than the MT-9F arrangement, which used nine MTM cells. Specifically, the T-shaped configuration, placed between the T_x and R_x coils, enhanced the PTE by 7.7%. This was because the T-shaped configuration focused the electromagnetic waves into specific regions, which led to a more confined power transfer channel, reducing energy loss and improving power transfer efficiency.

This finding suggests that a T-shaped MTM arrangement can improve WPT efficiency significantly, making it a promising option for future EV charging systems. These results underscore the importance of both the number and arrangement of MTM cells in optimizing WPT.

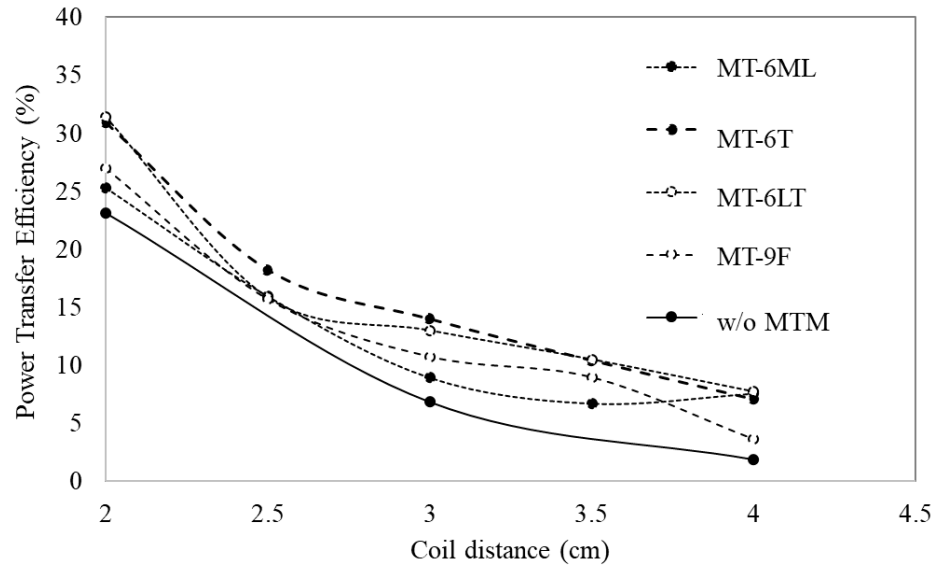


Figure 13. Relationship between coil distance and PTE for MT-6LT, MT-6T, MT-6ML, and MT-9F models.

5. Conclusions

This research investigates and improves WPT efficiency through both simulation and experimental studies, focusing on the use of an MTM placed between the T_x and R_x coils. The MTM model is validated against referenced studies and specifically designed to operate at 85 kHz. We examine the performance of the WPT system with the designed MTM, showing that the inclusion of the MTM resulted in higher PTE compared to systems without MTM. This improvement was attributed to the MTM's ability to align the magnetic field and increase the magnetic flux density at the receiver coil.

This study explored various MTM cell arrangements and numbers of cells, with MTM cells positioned at left, right, top, and bottom locations. The results indicated that the arrangement of six MTM cells provided the highest PTE compared to arrangements with three or nine MTM cells. This was due to the optimal quantity and distribution of electromagnetic flux, which was significantly influenced by the positioning and number of MTM cells. The maximum PTE was achieved with a T-shaped arrangement of six MTM cells at a coil distance of 2.0 cm.

Although the number of MTM cells influences PTE, the distribution of electromagnetic flux also plays a crucial role in the overall efficiency. The T-shaped arrangement of six MTM cells demonstrated a 7.7% improvement in PTE compared to the nine-cell arrangement. This T-shaped MTM configuration holds promise for enhancing WPT efficiency, offering a potential solution for future EV charging systems.

Author Contributions: Conceptualization, W.O. and A.K.; methodology, W.O. and A.K.; validation, S.P., S.T. and N.W.; formal analysis, W.O. and A.K.; investigation S.P., S.T. and N.W.; resources, W.O. and A.K.; data curation, S.P., S.T. and N.W.; writing—original draft preparation, S.P., S.T. and N.W.; writing—review and editing, W.O. and A.K.; visualization, W.O., S.P., S.T., N.W. and A.K.; supervision, W.O. and A.K.; project administration, A.K.; funding acquisition, W.O. and A.K. All authors have read and agreed to the published version of the manuscript.

Funding: This research received no external funding.

Data Availability Statement: The original contributions presented in the study are included in the article, further inquiries can be directed to the corresponding author.

Acknowledgments: The authors would like to express their sincere gratitude to Manop Masomtob from National Energy Technology Center (ENTEC), National Science and Technology Development Agency (NSTDA), for his academic and practical support. The authors are also grateful to the Department of Mechanical Engineering, Faculty of Engineering, and Department of Physics, Faculty of Science, King Mongkut's University of Technology Thonburi (KMUTT), for providing financial support and necessary facilities.

Conflicts of Interest: The authors declare no conflict of interest.

References

1. EEA. Greenhouse Gas Emissions from Transport in Europe. 2024. Available online: <https://www.eea.europa.eu/en/analysis/indicators/greenhouse-gas-emissions-from-transport> (accessed on 5 November 2024).
2. EEA. 2021. Available online: <https://www.eea.europa.eu/en/topics/in-depth/transport-and-mobility> (accessed on 27 October 2024).
3. European Environment Agency. Electric Vehicles in Europe. 2016. Available online: <https://www.eea.europa.eu/en/analysis/publications/electric-vehicles-in-europe> (accessed on 27 October 2024).
4. Del Pero, F.; Delogu, M.; Pierini, M. Life Cycle Assessment in the automotive sector: A comparative case study of Internal Combustion Engine (ICE) and electric car. *Procedia Struct. Integr.* **2018**, *12*, 521–537. [CrossRef]
5. Peng, T.; Ou, X.; Yan, X. Development and application of an electric vehicle's life-cycle energy consumption and greenhouse gas emissions analysis model. *Chem. Eng. Res. Des.* **2018**, *131*, 699–708. Available online: <https://www.eea.europa.eu> (accessed on 27 February 2022). [CrossRef]
6. Koengkan, M.; Fuinhas, J.A.; Teixeira, M.; Kazemzadeh, E.; Auza, A.; Dehdar, F.; Osmani, F. The Capacity of Battery-Electric and Plug-in Hybrid Electric Vehicles to Mitigate CO₂ Emissions: Macroeconomic Evidence from European Union Countries. *World Electr. Veh. J.* **2022**, *13*, 58. [CrossRef]
7. Kene, R.O.; Olwal, T.O. Energy Management and Optimization of Large-Scale Electric Vehicle Charging on the Grid. *World Electr. Veh. J.* **2023**, *14*, 95. [CrossRef]
8. Song, M.; Jayathurathnage, P.; Zanganeh, E.; Krasikova, M.; Smirnov, P.; Belov, P.; Kapitanova, P.; Simovski, S.; Krasnok, A. Wireless power transfer based on novel physical concepts. *Nat. Electron.* **2021**, *4*, 707–716. [CrossRef]
9. Yu, L.; Lin, P. Hardware Architecture of Wireless Power Transfer, RFID and WIPT System. *arXiv* **2024**, arXiv:2102.06876v1.
10. Wisartpong, P. A review of wireless power transfer. *Eng. Trans.* **2021**, *24*, 161–169.
11. Lerosey, G. Wireless power on the move. *Nature* **2017**, *546*, 354–355. [CrossRef] [PubMed]
12. Kodeeswaran, S.; Nandhini Gayathri, M.; Peña-Alzola, R.; Sanjeevikumar, P.; Prasad, R. Electric Vehicle Wireless Charging—Design and Analysis Using Circuit Capacitive Coupler. 2017. Available online: <https://Shorturl.asia/tDfSz> (accessed on 20 October 2024).
13. Pham, T.S.; Nguyen, T.D.; Tung, B.S.; Khuyen, B.X.; Hoang, T.T.; Ngo, Q.M.; Hiep, L.T.H.; Lam, V.D. Optimal frequency for magnetic resonant wireless power transfer in conducting medium. *Sci. Rep.* **2021**, *11*, 1–11. [CrossRef] [PubMed]
14. Alhamrouni, I.; Iskandar, M.; Salem, M.; Awal, L.J.; Jusoh, A.; Sutikno, T. Application of inductive coupling for wireless power transfer. *Int. J. Power Electron. Drive Syst.* **2020**, *11*, 1109–1116. [CrossRef]
15. Zhou, H.; Zhu, B.; Hu, W.; Liu, Z.; Gao, X. Modelling and practical implementation of 2-Coil wireless power transfer systems. *J. Electr. Comput. Eng.* **2014**, *1*, 906537. [CrossRef]
16. Bouanou, T.; Fadil, H.E.; Lassioui, A.; Assaddiki, O.; Njili, S. Analysis of Coil Parameters and Comparison of Circular, Rectangular, and Hexagonal Coils Used in WPT System for Electric Vehicle Charging. *World Electr. Veh. J.* **2021**, *12*, 45. [CrossRef]
17. Nalinnopphakhun, P.; Onreabroy, W.; Kaewpradap, A. Parameter Effects on Induction Coil Transmitter of Wireless Charging Systems for Small Electric Motorcycle. In Proceedings of the 2018 IEEE International WIE Conference on Electrical and Computer Engineering (WIECON-ECE), Chonburi, Thailand, 14–16 December 2018; IEEE: Bangkok, Thailand, 2018. [CrossRef]
18. Lee, W.S.; Oh, K.-S.; Yu, J.W. Distance-insensitive wireless power transfer and nearfield communication using a current-controlled loop with a loaded capacitance. *IEEE Trans. Antennas Propag.* **2014**, *62*, 936–940. [CrossRef]
19. Bevacqua, M.T.; Bellizzi, G.G.; Merenda, M. An efficient far-field wireless power transfer via field intensity shaping techniques. *Electronics* **2021**, *10*, 1609. [CrossRef]
20. Vatsala, V.; Alam, M.S.; Ahmad, A.; Chaban Rakan, C. Efficiency Enhancement of Wireless Charging for Electric Vehicles Through Reduction of Coil Misalignment. In Proceedings of the IEEE Transportation Electrification Conference and Expo (ITEC), Chicago, IL, USA, 22–24 June 2017; pp. 1–6.
21. Lee, W.; Yoon, Y. Wireless Power Transfer Systems Using Metamaterials, University of Florida. *IEEE Access* **2020**, *8*, 147930–147947. [CrossRef]
22. Amasiri, W.; Pijitrojana, W. Metamaterials for Optimizing Wireless Power Transfer. *J. Sci. Technol.* **2018**, *27*, 361–379. [CrossRef]
23. Smith, D.R.; Vier, D.C.; Koschny, T.; Soukoulis, C.M. Electromagnetic parameter retrieval from inhomogeneous metamaterials, Physical Review E 25th Anniversary Milestones. *Phys. Rev. E* **2005**, *71*, 036617. [CrossRef] [PubMed]

24. Li, G.; Lang, L.; Ren, J.; Fang, K.; Sun, Y.; Zhang, Y.; Li, Y.; Chen, H. Designment of wireless power transmitting system with magnetic megahertz metamaterials. In Proceedings of the IEEE Wireless Power Transfer Conference (WPTC), London, UK, 18–21 June 2019. [[CrossRef](#)]
25. Smith, D.R.; Padilla, W.J.; Vier, D.C.; Nemat-Nasser, S.C.; Schultz, S. Composite Medium with Simultaneously Negative Permeability and Permittivity. *Phys. Rev. Lett.* **2000**, *84*, 4184. [[CrossRef](#)] [[PubMed](#)]
26. Pendry, J.B.; Holden, A.J.; Robbins, D.J.; Stewart, W.J. Magnetism from conductors and enhanced nonlinear phenomena. Microwave theory and Techniques. *IEEE Trans. Microw. Theory Tech.* **1999**, *47*, 2075–2084. [[CrossRef](#)]
27. Li, W.; Wang, P.; Yao, C.; Zhang, Y.; Tang, H. Experimental investigation of 1D, 2D, and 3D metamaterials for efficiency enhancement in a 6.78MHz wireless power transfer system. In Proceedings of the IEEE Wireless Power Transfer Conference (WPTC), Aveiro, Portugal, 5–6 May 2016.
28. Smith, D.R.; Schilling, J.R. Resonant Metamaterials: The Role of Split-Ring Resonators in Magnetic Field Enhancement. *J. Appl. Phys.* **2007**, *102*, 094503.

Disclaimer/Publisher’s Note: The statements, opinions and data contained in all publications are solely those of the individual author(s) and contributor(s) and not of MDPI and/or the editor(s). MDPI and/or the editor(s) disclaim responsibility for any injury to people or property resulting from any ideas, methods, instructions or products referred to in the content.